Supplementary Material - A Three-Dimensional Numerical Model of an Active Cell Cortex in the Viscous Limit

Christian Bächer [1], Diana Khoromskaia [2], Guillaume Salbreux [2,3] and Stephan Gekle [1]

[1]Biofluid Simulation and Modeling, Theoretische Physik VI, Department of Physics, University of Bayreuth, Bayreuth, Germany
[2]The Francis Crick Institute, London, UK
[3]Department of Genetics and Evolution, University of Geneva, Geneva, Switzerland

S1 Velocity derivatives by an inversion of the parabolic fitting

A key step of the developed method is the expression of the local derivative of the velocity vector by means of the velocity evaluated at the nodes of the numerical mesh, as detailed in section 3.5 of the main part. This can be directly used to replace the velocity derivatives in the force balance equations such that we end up with a system of equations that is solvable for the velocities. In the following, we provide details on the analytical procedure behind this important step. As illustrated by equation (48) in the main part we use a parabolic fitting procedure of the velocity vector in the vicinity of each node, which we invert analytically. This in turn results in the velocity derivatives $\boldsymbol{A}_v, \boldsymbol{B}_v, \ldots, \boldsymbol{E}_v$ evaluated at a node in terms of the velocity vectors of the node $\boldsymbol{r}_\nu$ and its N_ν neighboring nodes, which are referred to by $a(\nu)$. With the differential form of equation (48)

$$\mathrm{d}(\chi_v^2) = \sum_i \sum_{a=1}^{N_\nu} 2\left(\bar{\boldsymbol{v}} - \boldsymbol{v}_a\right)_i \, \mathrm{d}v_i, \tag{S1.1}$$

we are able to minimize χ_v^2 with respect to the components of the fitting coefficients, e.g., A_v^j

$$\frac{\partial(\chi_v^2)}{\partial A_v^j} = \sum_i \sum_a 2\left(\bar{\boldsymbol{v}} - \boldsymbol{v}_a\right)_i \underbrace{\frac{\partial \bar{v}_i}{\partial A_v^j}}_{\xi\delta_{ij}} = \sum_a 2\left(\bar{\boldsymbol{v}} - \boldsymbol{v}_a\right)_j \xi \overset{!}{=} 0. \tag{S1.2}$$

Here, we clearly see that each component $j = x, y, z$ is minimized individually. Performing the minimization by calculating all derivatives with respect to $\boldsymbol{A}_v, \ldots, \boldsymbol{E}_v$ we end up with a system of linear equations with $\boldsymbol{A}_v, \boldsymbol{B}_v, \ldots, \boldsymbol{E}_v$ building the solution vector. By solving this system we obtain $\boldsymbol{A}_v, \boldsymbol{B}_v, \ldots, \boldsymbol{E}_v$ in terms of the velocity evaluated at the central and neighbor nodes.

We solve this system of linear equations analytically as detailed below. Since each velocity component can be treated separately, we illustrate the procedure in the following for a scalar fitting parameter only.

We consider a parabolic expansion of a quantity f around a central node $\boldsymbol{r}_\nu$ in its local coordinates (ξ, η). At the position of the neighbors a the expansion should be equal to the actual value of the function f

evaluated at the neighboring nodes as in equation (48)

$$\bar{f}_\nu(\xi_a, \eta_a) = f_\nu + P_{\nu a} \stackrel{!}{=} f_{a(\nu)}, \tag{S1.3}$$

with

$$P_{\nu a} = A\xi_a + B\eta_a + \frac{1}{2}C\xi_a^2 + \frac{1}{2}D\eta_a^2 + E\xi_a\eta_a. \tag{S1.4}$$

We consider a χ_f^2 analogous to equation (48) and proceed as in equation (S1.2) with a minimization of χ_f^2 to obtain

$$\begin{aligned}
\frac{\partial}{\partial A}\left(\chi_f^2\right) &= 2\sum_i \left[f_{a(\nu)} - \bar{f}_\nu(\xi_a, \eta_a)\right]\xi_a = 0, \\
\frac{\partial}{\partial B}\left(\chi_f^2\right) &= 2\sum_i \left[f_{a(\nu)} - \bar{f}_\nu(\xi_a, \eta_a)\right]\eta_a = 0, \\
\frac{\partial}{\partial C}\left(\chi_f^2\right) &= 2\sum_i \left[f_{a(\nu)} - \bar{f}_\nu(\xi_a, \eta_a)\right]\frac{1}{2}\xi_a^2 = 0, \\
\frac{\partial}{\partial D}\left(\chi_f^2\right) &= 2\sum_i \left[f_{a(\nu)} - \bar{f}_\nu(\xi_a, \eta_a)\right]\frac{1}{2}\eta_a^2 = 0, \\
\frac{\partial}{\partial E}\left(\chi_f^2\right) &= 2\sum_i \left[f_{a(\nu)} - \bar{f}_\nu(\xi_a, \eta_a)\right]\xi_a\eta_a = 0.
\end{aligned}$$

Re-writing these equations using equation (S1.3) we get

$$\begin{aligned}
\sum_a P_{\nu a}\xi_a &= \sum_a \left(f_{a(\nu)} - f_\nu\right)\xi_a, \\
\sum_a P_{\nu a}\eta_a &= \sum_a \left(f_{a(\nu)} - f_\nu\right)\eta_a, \\
\sum_a P_{\nu a}\frac{1}{2}\xi_a^2 &= \sum_a \left(f_{a(\nu)} - f_\nu\right)\frac{1}{2}\xi_a^2, \\
\sum_a P_{\nu a}\frac{1}{2}\eta_a^2 &= \sum_a \left(f_{a(\nu)} - f_\nu\right)\frac{1}{2}\eta_a^2, \\
\sum_a P_{\nu a}\xi_a\eta_a &= \sum_a \left(f_{a(\nu)} - f_\nu\right)\xi_i\eta_a.
\end{aligned}$$

Inserting (S1.4) we obtain for example for the first equation

$$(\sum_a \xi_a^2)A + (\sum_a \eta_a\xi_a)B + (\sum_a \frac{1}{2}\xi_a^3)C + (\sum_a \frac{1}{2}\eta_a^2\xi_a)D + (\sum_a \eta_a\xi_a^2)E = \sum_a (f_{a(\nu)} - f_\nu)\xi_a. \tag{S1.5}$$

Taking all equations together and using the separation with respect to the fitting coefficients we obtain a system of linear equations

$$\boldsymbol{\alpha} \cdot \begin{pmatrix} A \\ B \\ C \\ D \\ E \end{pmatrix} = \begin{pmatrix} \sum_a (f_{a(\nu)} - f_\nu)\xi_a \\ \sum_a (f_{a(\nu)} - f_\nu)\eta_a \\ \sum_a (f_{a(\nu)} - f_\nu)\frac{1}{2}\xi_a^2 \\ \sum_a (f_{a(\nu)} - f_\nu)\frac{1}{2}\eta_a^2 \\ \sum_a (f_{a(\nu)} - f_\nu)\xi_a\eta_a \end{pmatrix} = \boldsymbol{r}_s, \tag{S1.6}$$

with $\boldsymbol{r}_s$ denoting the right hand side and the symmetric 5×5 matrix $\boldsymbol{\alpha}$, i.e., $\alpha_{mn} = \alpha_{lm}$ with $m, n = 1, \ldots, 5$, being

$$\begin{pmatrix} \alpha_{11} = \sum\limits_a \xi_a^2 & & & & \\ \alpha_{12} = \sum\limits_a \xi_a\eta_a & \alpha_{22} = \sum\limits_a \eta_a^2 & & \alpha_{mn} = \alpha_{lm} & \\ \alpha_{13} = \sum\limits_a \frac{1}{2}\xi_a^3 & \alpha_{23} = \sum\limits_a \frac{1}{2}\xi_a^2\eta_a & \alpha_{33} = \sum\limits_a \frac{1}{4}\xi_a^4 & & \\ \alpha_{14} = \sum\limits_a \frac{1}{2}\xi_a\eta_a^2 & \alpha_{24} = \sum\limits_a \frac{1}{2}\eta_a^3 & \alpha_{34} = \sum\limits_a \frac{1}{4}\xi_a^2\eta_a^2 & \alpha_{44} = \sum\limits_a \frac{1}{4}\eta_a^4 & \\ \alpha_{15} = \sum\limits_a \xi_a^2\eta_a & \alpha_{25} = \sum\limits_a \xi_a\eta_a^2 & \alpha_{35} = \sum\limits_a \frac{1}{2}\xi_a^3\eta_a & \alpha_{45} = \sum\limits_a \frac{1}{2}\xi_a\eta_a^3 & \alpha_{55} = \sum\limits_a \xi_a^2\eta_a^2 \end{pmatrix}. \tag{S1.7}$$

By inverting the matrix $\boldsymbol{\alpha}$ to $\boldsymbol{\beta} = \boldsymbol{\alpha}^{-1}$ we can obtain the fitting parameters by

$$\begin{pmatrix} A \\ B \\ C \\ D \\ E \end{pmatrix} = \boldsymbol{\beta} \cdot \boldsymbol{r}_s. \tag{S1.8}$$

Using Mathematica, we obtain the inverse of a general symmetric 5×5 matrix $\boldsymbol{\alpha}$ with entries α_{mn}, which we term β_{mn}. Inserting the actual values α_{mn} as given above, we calculate the numerical elements of the inverse matrix β_{mn}.

With the inverse matrix and using equation (S1.8) we obtain the fitting coefficients

$$A = \sum_{n=1}^{5} \beta_{1n} r_{sn} = A(\{f_\mu\}), \tag{S1.9}$$

$$B = \sum_{n=1}^{5} \beta_{2n} r_{sn} = B(\{f_\mu\}), \tag{S1.10}$$

$$C = \sum_{n=1}^{5} \beta_{3n} r_{sn} = C(\{f_\mu\}), \tag{S1.11}$$

$$D = \sum_{n=1}^{5} \beta_{4n} r_{sn} = D(\{f_\mu\}), \tag{S1.12}$$

$$E = \sum_{n=1}^{5} \beta_{5n} r_{sn} = E(\{f_\mu\}), \tag{S1.13}$$

as functions of the quantity f evaluated at the nodes, i.e., of the set $\{f_\mu\}$. Thus, $A, B, \ldots, E$ are linear combinations of the function values, in particular of the vales at the central node ν and its neighbors. As a consequence the derivatives $\frac{\partial}{\partial f_\mu} A$, which are required for the minimization ansatz, can easily be calculated.

In order to calculate the derivatives we re-write the expressions for the coefficients. Using the definition of $\boldsymbol{r}_s$ in eq. (S1.6) we obtain

$$\begin{aligned} A =& \sum_a \underbrace{\left(\beta_{11}\xi_a + \beta_{12}\eta_a + \beta_{13}\frac{1}{2}\xi_a^2 + \beta_{14}\frac{1}{2}\eta_a^2 + \beta_{15}\xi_a\eta_a \right)}_{p_a^A} f_a + \\ & \underbrace{(-1)\left[\beta_{11}\left(\sum \xi_a\right) + \beta_{12}\left(\sum \eta_a\right) + \beta_{13}\left(\sum \frac{1}{2}\xi_a^2\right) + \beta_{14}\left(\sum \frac{1}{2}\eta_a^2\right) + \beta_{15}\left(\sum \xi_a\eta_a\right)\right]}_{p_\nu^A} f_\nu, \end{aligned}$$

$$\begin{aligned} B =& \sum_a \left(\beta_{12}\xi_a + \beta_{22}\eta_a + \beta_{23}\frac{1}{2}\xi_a^2 + \beta_{24}\frac{1}{2}\eta_a^2 + \beta_{25}\xi_a\eta_a \right) f_a + \\ & (-1)\left[\beta_{12}\left(\sum \xi_a\right) + \beta_{22}\left(\sum \eta_a\right) + \beta_{23}\left(\sum \frac{1}{2}\xi_a^2\right) + \beta_{24}\left(\sum \frac{1}{2}\eta_a^2\right) + \beta_{25}\left(\sum \xi_a\eta_a\right)\right] f_\nu, \end{aligned}$$

$$\begin{aligned} C =& \sum_a \left(\beta_{13}\xi_a + \beta_{23}\eta_a + \beta_{33}\frac{1}{2}\xi_a^2 + \beta_{34}\frac{1}{2}\eta_a^2 + \beta_{35}\xi_a\eta_a \right) f_a + \\ & (-1)\left[\beta_{13}\left(\sum \xi_a\right) + \beta_{23}\left(\sum \eta_a\right) + \beta_{33}\left(\sum \frac{1}{2}\xi_a^2\right) + \beta_{34}\left(\sum \frac{1}{2}\eta_a^2\right) + \beta_{35}\left(\sum \xi_a\eta_a\right)\right] f_\nu, \end{aligned}$$

$$D = \sum_a \left(\beta_{14}\xi_a + \beta_{24}\eta_a + \beta_{34}\frac{1}{2}\xi_a^2 + \beta_{44}\frac{1}{2}\eta_a^2 + \beta_{45}\xi_a\eta_a \right) f_a +$$
$$(-1)\left[\beta_{14}\left(\sum \xi_a\right) + \beta_{24}\left(\sum \eta_a\right) + \beta_{34}\left(\sum \frac{1}{2}\xi_a^2\right) + \beta_{44}\left(\sum \frac{1}{2}\eta_a^2\right) + \beta_{45}\left(\sum \xi_a\eta_a\right) \right] f_\nu,$$

$$E = \sum_a \left(\beta_{15}\xi_a + \beta_{25}\eta_a + \beta_{35}\frac{1}{2}\xi_a^2 + \beta_{45}\frac{1}{2}\eta_a^2 + \beta_{55}\xi_a\eta_a \right) f_a +$$
$$(-1)\left[\beta_{15}\left(\sum \xi_a\right) + \beta_{25}\left(\sum \eta_a\right) + \beta_{35}\left(\sum \frac{1}{2}\xi_a^2\right) + \beta_{45}\left(\sum \frac{1}{2}\eta_a^2\right) + \beta_{55}\left(\sum \xi_a\eta_a\right) \right] f_\nu.$$

Using the notation indicated in the first line, we can write

$$\begin{aligned} A &= \sum_a p_a^A f_a + p_\nu^A f_\nu, \\ B &= \sum_a p_a^B f_a + p_\nu^B f_\nu, \\ C &= \sum_a p_a^C f_a + p_\nu^C f_\nu, \\ D &= \sum_a p_a^D f_a + p_\nu^D f_\nu, \\ E &= \sum_a p_a^E f_a + p_\nu^E f_\nu. \end{aligned} \tag{S1.14}$$

The prefactors in front of f_ν and f_a, respectively, are the derivatives of the coefficients with respect to f_μ (in case of $\mu = \nu$ and $\mu = a(\nu)$, respectively).

S2 Analytical solution for flows on a sphere in terms of spherical harmonics

In the following, we derive an analytical solution for the spherical cortex of radius R with an active surface stress distribution in terms of spherical harmonics as given by equation (50). Here, the coordinates with Greek letter index α, β, γ refer to the spherical coordinates on a sphere (θ, ϕ), such that a point on the sphere is given by

$$\boldsymbol{X}(\theta, \phi) = R\left[\sin\theta\cos\phi\boldsymbol{e}_x + \sin\theta\sin\phi\boldsymbol{e}_y + \cos\theta\boldsymbol{e}_z\right]. \tag{S2.1}$$

The corresponding tangent vectors in eq. (1) on the sphere are given by

$$\boldsymbol{e}_\theta = \partial_\theta\boldsymbol{X} = R\left[\cos\theta\cos\phi\boldsymbol{e}_x + \cos\theta\sin\phi\boldsymbol{e}_y - \sin\theta\boldsymbol{e}_z\right] \tag{S2.2}$$
$$\boldsymbol{e}_\phi = \partial_\phi\boldsymbol{X} = R\left[-\sin\theta\sin\phi\boldsymbol{e}_x + \sin\theta\cos\phi\boldsymbol{e}_y\right]. \tag{S2.3}$$

The metric in eq. (3) evaluates to

$$g_{\alpha\beta} = R^2 \begin{pmatrix} 1 & 0 \\ 0 & \sin^2\theta \end{pmatrix} \tag{S2.4}$$

and the curvature tensor in eq. (4) is $C_\alpha{}^\beta = \frac{1}{R}\delta_\alpha^\beta$. In the following, we also use the Levi-Civita tensor on the surface, defined by

$$\epsilon_{\alpha\beta} = (\boldsymbol{e}_\alpha \times \boldsymbol{e}_\beta) \cdot \boldsymbol{n}. \tag{S2.5}$$

Spherical harmonics. We now discuss briefly scalar, vector and tensorial spherical harmonics. The spherical harmonics expansion of a general scalar field on the sphere $f(\theta, \phi)$ reads

$$f(\theta, \phi) = \sum_{l=0}^{\infty} \sum_{m=-l}^{l} f_{lm} Y_{lm}(\theta, \phi), \tag{S2.6}$$

where the spherical harmonics

$$Y_{lm}(\theta, \phi) = \alpha_{lm} P_l^m(\cos\theta) e^{im\phi}, \tag{S2.7}$$

with $P_l^m(x)$ the associated Legendre polynomials, are eigenfunctions of the Laplace equation on the sphere

$$R^2 \nabla_\alpha \nabla^\alpha Y_{lm} = -l(l+1) Y_{lm}. \tag{S2.8}$$

The coefficients α_{lm} are given by

$$\alpha_{lm} = \sqrt{\frac{(2l+1)(l-m)!}{4\pi(l+m)!}} \tag{S2.9}$$

so that the orthonormality condition

$$\int\limits_{\theta=0}^{\theta=\pi} \int\limits_{\phi=0}^{\phi=2\pi} Y_{lm} Y_{l'm'}^* \sin\theta d\theta d\phi = \delta_{ll'} \delta_{mm'}, \tag{S2.10}$$

where the asterisk denotes complex conjugation, is satisfied.

A general tangent vector field $\boldsymbol{a}$ on the sphere admits an expansion in terms of vectorial spherical harmonics (Barrera et al., 1985)

$$\boldsymbol{a} = \sum_{l,m} a_{lm}^1 \boldsymbol{s}_{lm}^1 + a_{lm}^2 \boldsymbol{s}_{lm}^2, \tag{S2.11}$$

where we now use the short-hand notation (l, m) for summation over spherical harmonics. The vectorial spherical harmonics $\boldsymbol{s}_{lm}^1$, $\boldsymbol{s}_{lm}^2$ are defined by:

$$\begin{aligned} \boldsymbol{s}_{lm}^1 &= R(\partial_\alpha Y_{lm}) \boldsymbol{e}^\alpha \\ \boldsymbol{s}_{lm}^2 &= \boldsymbol{n} \times \boldsymbol{s}_{lm}^1 = R\epsilon^{\alpha\beta}(\partial_\alpha Y_{lm}) \boldsymbol{e}_\beta. \end{aligned}$$

For a non-tangent vector field, the normal component is a scalar field which itself can be expanded in spherical harmonics according to eq. (S2.6).

We also use the following definition of traceless symmetric tensorial spherical harmonics

$$
\begin{aligned}
S^{1,\alpha\beta}_{lm} =& \frac{R^2}{2}[\nabla^\alpha\nabla^\beta + \nabla^\beta\nabla^\alpha - g^{\alpha\beta}\nabla_\gamma\nabla^\gamma]Y_{lm}\\
S^{2,\alpha\beta}_{lm} =& \frac{R^2}{2}[\epsilon^{\gamma\alpha}\nabla^\beta\nabla_\gamma + \epsilon^{\gamma\beta}\nabla^\alpha\nabla_\gamma]Y_{lm}.
\end{aligned} \tag{S2.12}
$$

Using eq. (S2.8), one can verify that the tensorial spherical harmonics satisfy the following identities

$$\nabla_\alpha\nabla_\beta S^{1,\alpha\beta}_{lm} = \frac{l(l+1)}{2R^2}(l(l+1)-2)Y_{lm} \tag{S2.13}$$

$$\epsilon^\beta{}_\alpha\nabla_\beta\nabla_\gamma S^{1,\gamma\alpha}_{lm} = 0 \tag{S2.14}$$

$$\nabla_\alpha\nabla_\beta S^{2,\alpha\beta}_{lm} = 0 \tag{S2.15}$$

$$\epsilon^\beta{}_\alpha\nabla_\beta\nabla_\gamma S^{2,\gamma\alpha}_{lm} = \frac{l(l+1)}{2R^2}(l(l+1)-2)Y_{lm}. \tag{S2.16}$$

Active surface stress driven flows on a sphere. We now consider flows on a sphere driven by the isotropic active surface stress $\zeta(\theta,\phi)g_{\alpha\beta}$ in eq. (49). The isotropic active stress $\zeta(\theta,\phi)$ can be expanded in spherical harmonics according to equation (50).

The velocity field $\boldsymbol{v}$ has a normal component which can be expanded in spherical harmonics and a tangential part which can be expanded in vector spherical harmonics such that the velocity becomes

$$\boldsymbol{v} = \sum_{l,m}\left[v^1_{lm}\boldsymbol{s}^1_{lm} + v^2_{lm}\boldsymbol{s}^2_{lm} + v^n_{lm}Y_{lm}\boldsymbol{n}\right], \tag{S2.17}$$

where dependencies on θ,ϕ have been omitted for compactness of the notation. Here, we use the convention $v^1_{00} = v^2_{00} = 0$ as $\boldsymbol{s}^1_{00} = \boldsymbol{s}^2_{00} = 0$.

We now aim to relate the coefficients of the velocity expansion v^1_{lm}, v^2_{lm} and v^n_{lm} to the coefficients of the active surface stress expansion ζ_{lm}. For this, we first note that the viscous part of the surface stress tensor defined by eq. (15)

$$t_{v,\alpha\beta} = 2\eta_s\left(\frac{1}{2}\left[\nabla_\alpha v_\beta + \nabla_\beta v_\alpha\right] + C_{\alpha\beta}v^n - \frac{1}{2}g_{\alpha\beta}\nabla_\gamma v^\gamma - \frac{1}{2}g_{\alpha\beta}C^\gamma_\gamma v^n\right) + \eta_b(\nabla_\gamma v^\gamma + C^\gamma_\gamma v^n)g_{\alpha\beta} \tag{S2.18}$$

has an expansion in terms of spherical harmonics of the following form

$$t^{\alpha\beta}_v = \frac{2\eta_s}{R}\sum_{l,m}[v^1_{lm}S^{1,\alpha\beta}_{lm} + v^2_{lm}S^{2,\alpha\beta}_{lm}] + \frac{\eta_b}{R}g^{\alpha\beta}\sum_{l,m}[-l(l+1)v^1_{lm} + 2v^n_{lm}]Y_{lm}, \tag{S2.19}$$

where we have used eq. (S2.8), the definition of the trace-less tensorial spherical harmonics in eq. (S2.12) and the expression for the curvature tensor on the sphere.

We now solve the three force balance equations, where the tangential ones are rewritten into two separate scalar equations

$$\nabla_\alpha \nabla_\beta t^{\alpha\beta} = 0 \tag{S2.20}$$

$$\epsilon^\gamma{}_\beta \nabla_\gamma \nabla_\alpha t^{\alpha\beta} = 0 \tag{S2.21}$$

$$t^{\alpha\beta} C_{\alpha\beta} = P. \tag{S2.22}$$

Projecting the force balance equations on spherical harmonics and using eq. (S2.8) and eqs. (S2.13) - (S2.16) we obtain

$$\left[\left(\frac{\eta_s}{\eta_b} + 1\right) l(l+1) - 2\frac{\eta_s}{\eta_b}\right] v^1_{lm} - 2v^n_{lm} = \frac{R\zeta_{lm}}{\eta_b} \tag{S2.23}$$

$$(l(l+1) - 2)v^2_{lm} = 0 \tag{S2.24}$$

$$l(l+1)v^1_{lm} - 2v^n_{lm} = \frac{R\zeta_{lm}}{\eta_b} - \frac{R^2 P_{lm}}{2\eta_b} \tag{S2.25}$$

where we have also introduced the decomposition of the pressure acting on the thin shell $P(\theta, \phi) = \sum\limits_{l,m} P_{lm} Y_{lm}(\theta, \phi)$. In the absence of an external net force on the sphere it applies $P_{1m} = 0$, which we assume is the case here.

For $l = 1$, the system is undetermined due to the invariance of the equations under solid translation and rotation. As detailed in section 3.2, the introduction of additional constraints for the motion of the center of the sphere and its solid rotation in eqs. (36) and (37) is required to completely solve for the velocity field. For $l > 1$, one has in general $v^2_{lm} = 0$.

Throughout the manuscript we consider a uniform pressure P_{00} and therefore we obtain for the zeroth-order of the spherical harmonics, i.e., $l = 0$, $m = 0$,

$$\frac{2\zeta_{00}}{R} + \frac{4\eta_b v^n_{00}}{R^2} = P_{00}. \tag{S2.26}$$

The incompressibility condition for the fluid inside the cell in eq. (35) implies $v^n_{00} = 0$ and the pressure is determined by the Laplace pressure $2\frac{\zeta_{00}}{\sqrt{4\pi}R}$ with $\frac{\zeta_{00}}{\sqrt{4\pi}}$ representing the constant average active surface stress. For higher order harmonics, $l > 1$, we obtain in that case $v^1_{lm} = 0$ and the normal velocity component

$$v^n_{lm} = -\frac{R\zeta_{lm}}{2\eta_b}. \tag{S2.27}$$

If we consider the case where the sphere can not deform, such that $v^n_{lm} = 0$, the normal force balance equation (S2.25) becomes an equation for the pressure field exerted by the surface with coefficients P_{lm}, and the tangential velocity field is given for $l > 1$ by

$$v^1_{lm} = \frac{R\zeta_{lm}}{(\eta_s + \eta_b)l(l+1) - 2\eta_s}. \tag{S2.28}$$

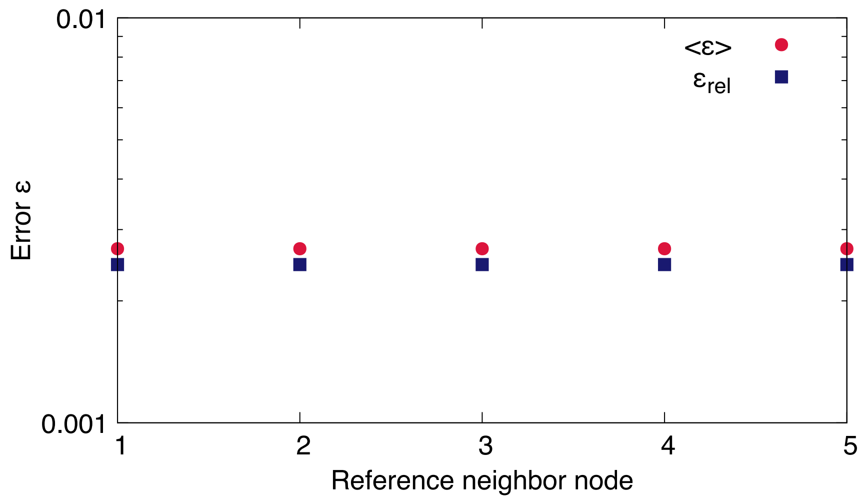

Figure S1. Variation of the reference neighboring node. The choice of the reference neighboring node, which serves for the construction of the local coordinate system, does not influence the numerical solution as illustrated by the constant error.

S3 Choice of reference neighbor does not affect results

As we detail in section 3.1 of the main part, for each node of the discretized thin shell representing the cell cortex a local coordinate system is constructed by use of one neighboring node as reference node. In order to prove evidence that this choice is arbitrary we consider the setup with non-axisymmetric active surface stress distribution in figure 3 of the main part with a fixed sphere discretized by 2562 nodes. Here, we systematically vary the reference neighbor node, run one simulation per reference neighbor node, and quantify the deviation to the analytical solution in terms of the errors defined in equations (57) and (58). Figure 13 shows a constant error for varying reference neighbor node. Therefore, we are able to conclude that the choice of the reference neighbor node for local coordinate system construction is arbitrary.

S4 Axisymmetric simulations

Here we briefly describe the simulation approach for an axisymmetric viscous active cortex that is used to generate the cell surface dynamics, to which the three-dimensional method is compared in section 4.2 (see figures 5, 7, and 8 in the main part). For more details on this numerical approach we refer to ref. (Khoromskaia and Salbreux, 2021).

In this approach we introduce a bending moment tensor

$$\bar{m}^{\alpha\beta} = \eta_{cb} \left(\frac{\mathrm{D}}{\mathrm{Dt}} C_\gamma^\gamma \right) g^{\alpha\beta}, \tag{S4.1}$$

with the corotational time derivative of the trace of the curvature tensor (Salbreux and Jülicher, 2017)

$$\frac{\mathrm{D}}{\mathrm{Dt}} C_\gamma^\gamma = \partial_t C_\gamma^\gamma + v^\delta \nabla_\delta C_\gamma^\gamma, \tag{S4.2}$$

where the trace of the corotational term vanishes. This choice of $\bar{m}^{\alpha\beta}$ provides an alternative way to introduce damping in changes to the surface mean curvature, similarly to the bending viscosities $\bar{\eta}$ and

$\bar{\eta}_b$ used in the three-dimensional method (see section 3.4 of the main part). Since η_{cb} is also chosen to be small, $\eta_{cb} = 10^{-6} R^2 \eta_s$, we expect that the two alternative damping contributions result in dynamics that are close to each other.

The surface stress tensor, or tension tensor, is taken as in Equations (14) and (15), with the transformation $t_{ij} \to t_{ij} + \frac{1}{2}(\bar{m}^{ik} C_k{}^j + \bar{m}^{jk} C_k{}^i)$. These additional terms contribute naturally when considering constitutive equations for a surface subjected to internal bending moments (Salbreux and Jülicher, 2017).

The force balance equations (12) and (13) are amended to include the moment tensor via the normal surface stress $t_n^\alpha = \nabla_\gamma \bar{m}^{\gamma\alpha}$,

$$\nabla_\alpha t^{\alpha\beta} + C_\alpha{}^\beta t_n^\alpha = 0 \tag{S4.3}$$

$$\nabla_\alpha t_n^\alpha - C_{\alpha\beta} t^{\alpha\beta} = -P. \tag{S4.4}$$

The axisymmetric cortex is parametrized by the arc length $s \in [0, L]$, with L the pole-to-pole perimeter, and the azimuthal angle $\phi \in [0, 2\pi]$ as

$$\mathbf{X}(\phi, s) = (x(s)\cos(\phi), x(s)\sin(\phi), z(s))\,. \tag{S4.5}$$

The arc length coordinate is chosen such that $g_{ss} = 1$. The metric tensor is diagonal and therefore diagonal components in mixed coordinates are equal, i.e. for a tensor $\mathbf{A}$, $A_s^s = A_s{}^s = A^s{}_s$ and $A_\phi^\phi = A_\phi{}^\phi = A^\phi{}_\phi$. In this parametrization the force balance equations (S4.3) and (S4.4), together with the constitutive equations (S4.1) and (14) and (15) given in the main text, become three second-order equations in s, one each for the velocity components v^s and v^n and the torque component $\bar{m}_s^s$, which can be rewritten as a system of first-order differential equations (see ref. (Khoromskaia and Salbreux, 2021) for more details). These differential equations are integrated numerically using the boundary value problem solver bvp4c by MATLAB, which implements a fourth-order collocation method on an adaptive spatial grid. For the solver we use the relative tolerance $\varepsilon_{rel} = 10^{-4}$ and the absolute tolerance $\varepsilon_{abs} = 10^{-6}$. For the examples considered here, this results in typical grid sizes of $N \approx 100$.

We use an isotropic active surface stress profile of the form

$$\zeta_s^s(s, \phi, t = 0) = \zeta_\phi^\phi(s, \phi, t = 0) = \zeta(s, \phi, t = 0) = \zeta_0 + \hat{\zeta} \exp\left(-\left(\frac{(s - \pi R/2)^2}{2\bar{\sigma}^2}\right)^{\bar{p}}\right), \tag{S4.6}$$

and the parameters relate to those in equation (59) as $s = R\theta$, $\bar{p} = p/2$, and $\bar{\sigma} = R(\sqrt{2}\sqrt[p]{\sigma})^{-1}$. Because the active surface stress profile is up-down symmetric with respect to the equator of the cortex, the equations are solved on the reduced interval $0 \leq s \leq \frac{L}{2}$. The required boundary conditions on the south pole are

$$v^s(0) = \partial^s v^n(0) = \partial_s \bar{m}_s^s(0) = 0. \tag{S4.7}$$

With the active surface stress profile up-down symmetry considered here, the flow field $\mathbf{v}(s)$ satisfies the symmetry condition $v_s(s) = -v_s(L - s)$ and $v_n(s) = v_n(L - s)$, and the bending moment tensor satisfies $\bar{m}_s^s(s) = \bar{m}_s^s(L - s)$. Therefore, by symmetry the boundary conditions at the equator can be written:

$$v^s\left(\frac{L}{2}\right) = \partial_s v^n\left(\frac{L}{2}\right) = \partial_s \bar{m}_s^s\left(\frac{L}{2}\right) = 0. \tag{S4.8}$$

The condition on v^s ensures that the cortex is not displaced in z-direction and therefore takes the role of the total velocity constraint (36), which in this setup reduces to $2\pi \int_0^L ds\, xv_z = 0$. The incompressibility constraint (35) is incorporated into the system of ode's in the form of an equation for the partial rate of volume change $v(s) = 2\pi \int_0^s ds'\, xv_n$ with the boundary conditions $v(0) = v(L/2) = 0$. The constraint (37) which reduces to $\int_S dS\, x^2 v_\phi = 0$, is automatically satisfied in the axisymmetric setup since $v_\phi = 0$.

At each time step the shape and all surface quantities, except for the active surface stress profile $\zeta(s, \phi, t)$, are updated in a Lagrangian frame via

$$\mathbf{X}'(s, \phi, t + \Delta t) = \mathbf{X}(s, \phi, t) + \mathbf{v}(s, \phi, t)\Delta t, \tag{S4.9}$$

using the full velocity vector $\mathbf{v} = v^s \mathbf{e}_s + v^n \mathbf{n}$. Subsequently, the surface is reparametrised to a new arc length parameter $s'(s)$, $\mathbf{X}'(s, \phi, t + \Delta t) \to \mathbf{X}'(s', \phi, t + \Delta t)$, which is calculated from the condition $g_{s's'} = 1$ on the updated surface. For comparison with the three-dimensional method we also calculate the relationship between the arc length parameters at t and $t + \Delta t$ based on a surface update in the Euler approach, $\mathbf{X}'(s_E, \phi, t + \Delta t) = \mathbf{X}(s_E, \phi, t) + v^n(s_E, \phi, t)\mathbf{n}\Delta t$, where s_E is the Euler coordinate. This second reparametrisation $s'(s_E)$ is used to update the active surface stress profile on the cortex as

$$\zeta'(s', \phi, t + \Delta t) = \zeta(s_E(s'), \phi, t), \tag{S4.10}$$

such that it evolves in the same way as described in section 4.2 of the main part. All surface quantities are passed to the next time step as spline interpolants. The time step in the simulation is $\Delta t = 10^{-4} t_a$.

REFERENCES

Barrera RG, Estevez GA, Giraldo J. Vector spherical harmonics and their application to magnetostatics. *European Journal of Physics* **6** (1985) 287–294. doi:10.1088/0143-0807/6/4/014.

Khoromskaia D, Salbreux G. Active morphogenesis of epithelial shells. *in preparation* (2021).

Salbreux G, Jülicher F. Mechanics of active surfaces. *Physical Review E* **96** (2017) 032404. doi:10.1103/PhysRevE.96.032404.